

THE USE OF POISSON TO CALCULATE THE EFFECT OF
MAGNETIZATION IN SUPERCONDUCTING MAGNETS*

S. Caspi, W.S. Gilbert, M. Helm, and L.J. Laslett

Lawrence Berkeley Laboratory
University of California
Berkeley, CA 94720

August 1985

*This work was supported by the Director, Office of Energy Research, Office of High Energy and Nuclear Physics, High Energy Physics Division, U.S. Dept. of Energy, under Contract No. DE-AC03-76SF00098.

THE USE OF POISSON TO CALCULATE THE EFFECT OF MAGNETIZATION IN SUPERCONDUCTING MAGNETS*

S. Caspi, W.S. Gilbert, M. Helm, and L.J. Laslett

Lawrence Berkeley Laboratory
University of California
Berkeley, CA 94720

INTRODUCTION

Magnetostatic problems solved by POISSON employ current and air regions as well as regions of nonlinear permeable iron. In many problems it is customary to set the permeability of the current regions identical to that of air and to introduce a permeability table (e.g. B-H) for the iron regions. If the conductor is made of a superconducting material, setting the permeability of the current regions equal to that of air is only an approximation. The existence of surface and bulk super-currents, which act partially to shield the superconductor's interior from the penetrating field, results in the superconductor acquiring a magnetization that in some cases cannot be ignored. Magnetization in superconducting dipole magnets influences the field uniformity. This effect is quite small at high fields ($H \gg H_p$; H_p = field at penetration) but introduces large harmonic coefficients at low fields where the magnitude of the magnetization is of the order of the applied field.

Magnetization of a superconducting material can be introduced into POISSON through a field dependent permeability table (in much the same way that iron characteristics are introduced). This can be done by representing the increasing and decreasing field characteristics by two independent magnetization curves. We have verified that superposition of a current and a magnetization table in the same region does not violate the code.

*This was supported by the Director, Office of Energy Research, Office of High Energy and Nuclear Physics, High Energy Physics Division, U.S. Dept. of Energy, under Contract No. DE-AC03-76SF00098.

A similar method for calculating magnetization effects was recently proposed by M. Kuchnir and E. Fisk at Fermilab. However, the method outlined here takes advantage of integrating magnetization effects into the field relaxation process and thereby avoiding some of the inaccuracies introduced by perturbation techniques. G. Morgan of BNL also has reported on the use of GFUN to calculate magnetization effects using a similar method.

We present here two examples. The first uses a linear and reversible magnetization curve for which an analytical solution is compared with that of POISSON. The second is a more realistic case where a measured magnetization curve of a superconducting cable is introduced into POISSON and results are compared with measurements.

EXAMPLE 1 - MAGNETIZATION OF A CURRENT CARRYING ANNULUS

Analytical Solution

We first analyze an arrangement (sketched below) in which a current I_0 flows, with constant current density, into an annulus of inner and outer radii a, b and returns as I_0 through the annulus center.

The 2D ring cross section area is:

$$A = \pi(b^2 - a^2)$$

The current density is:

$$J_0 = \frac{I_0}{\pi(b^2 - a^2)}$$

We make use of relations:

$$\oint H \, d\ell = \frac{4\pi}{10} I$$

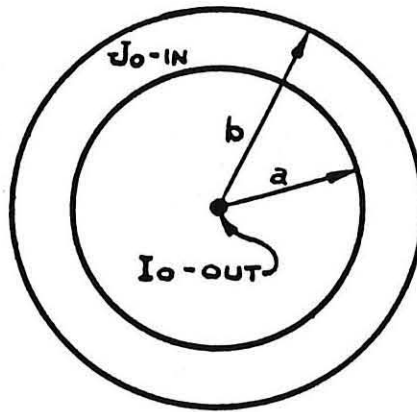
$$B = \mu_r H$$

$H = \text{Oersted}$

$\ell = \text{cm}$

$I = \text{Amp}$

$B = \text{Gauss}.$



Then, for $r < a$,

$$2\pi r H_{\theta} = \frac{4\pi}{10} I_0$$

$$H_{\theta} = \frac{2I_0}{10r} ;$$

For $b > r > a$,

$$I = I_0 - J_0 \pi(r^2 - a^2) = I_0 \frac{b^2 - r^2}{b^2 - a^2}$$

$$2\pi r H_{\theta} = \frac{4\pi}{10} I_0 \frac{b^2 - r^2}{b^2 - a^2}$$

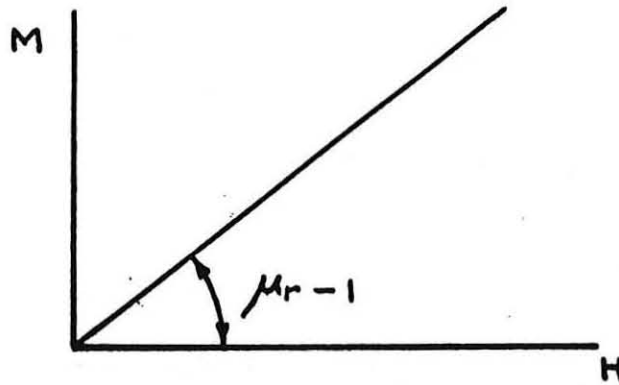
$$H_{\theta} = \frac{2I_0}{10} \frac{b^2 - r^2}{r(b^2 - a^2)}$$

$$B_{\theta} = \frac{2I_0}{10} \mu_r \frac{b^2 - r^2}{r(b^2 - a^2)} ;$$

and for $r > b$,

$$H_{\theta} = 0 .$$

If $\mu_r \neq 1$ in the ring, then $B \neq H$ - corresponding to a magnetization curve sketched below:



We now derive the vector potential A , using $B_\theta = -\partial A / \partial r$, so that it can be compared directly with POISSON's output.

For $r > b$: Since $A = \text{constant}$, we choose $A = 0$.

For $b > r > a$:

$$A = \frac{2I_0}{10} \mu_r \int_r^b \frac{b^2 - r^2}{r(b^2 - a^2)} dr$$

$$A = \frac{2I_0}{10} \mu_r \left[\frac{b^2}{b^2 - a^2} \ln \frac{b}{r} - \frac{1}{2} \frac{b^2 - r^2}{b^2 - a^2} \right]$$

and on $r = a$

$$A = \frac{2I_0}{10} \mu_r \left[\frac{b^2}{b^2 - a^2} \ln \frac{b}{a} - \frac{1}{2} \right].$$

For $r < a$:

$$A = A_{r=a} - \frac{2I_0}{10} \ln \frac{r}{a}$$

$$A = \frac{2I_0}{10} \left[\mu_r \left(\frac{b^2}{b^2 - a^2} \ln \frac{b}{a} - \frac{1}{2} \right) - \ln \frac{r}{a} \right].$$

If we select $a = 1$ cm, $b = 2$ cm, and $I_0 = 4000$ Amp, we calculate:

$$r \geq 2$$

$$A = 0$$

$$1 \leq r \leq 2$$

$$A = 800 \mu_r \left[\frac{4}{3} \ln \frac{2}{r} - \frac{4-r^2}{6} \right]$$

$$r \leq 1$$

$$A = 800 \left[\mu_r 0.424196 - \ln r \right]$$

In Table I below we compare numerical results for $\mu_r = 0.5$ and 1.5.

μ_r	r (cm)	A - analytical	A - Poisson	$\Delta\%$
0.5	0.5	724.20	723.3	0.12
	1.0	169.68	169.28	0.24
	1.5	36.76	36.6	0.45
1.5	0.5	1063.55	1062.3	0.12
	1.0	509.04	508.15	0.17
	1.5	110.29	110.0	0.26

EXAMPLE 2 - MAGNETIZATION OF A SUPERCONDUCTING DIPOLE MAGNET

Method and Application

We construct two groups of input tables for POISSON, intended to describe the magnetization of superconductor cables used in a dipole magnet [D-12C-2]. One group of tables includes all magnetization curves, of various cable types, during a field increase and the other provides similar curves for a decreasing field.

We require magnetization curves for the identical cables used in this magnet in order to take care of variations in strand size, copper to superconductor ratio, transport current, and critical current. The magnetization curve of an entire block and not of a single turn (or cable) will be required to take care of insulation, cable compactness,

small wedges, and other non-magnetic materials, since current regions in POISSON are usually represented by a single block rather than by a collection of individual turns.

In many cables measured magnetization curves may not be available and then the use of scaling may be required. The magnetization curve should be available over a range of field extending to values as high as the short-sample limit.

Magnet D-12C-2

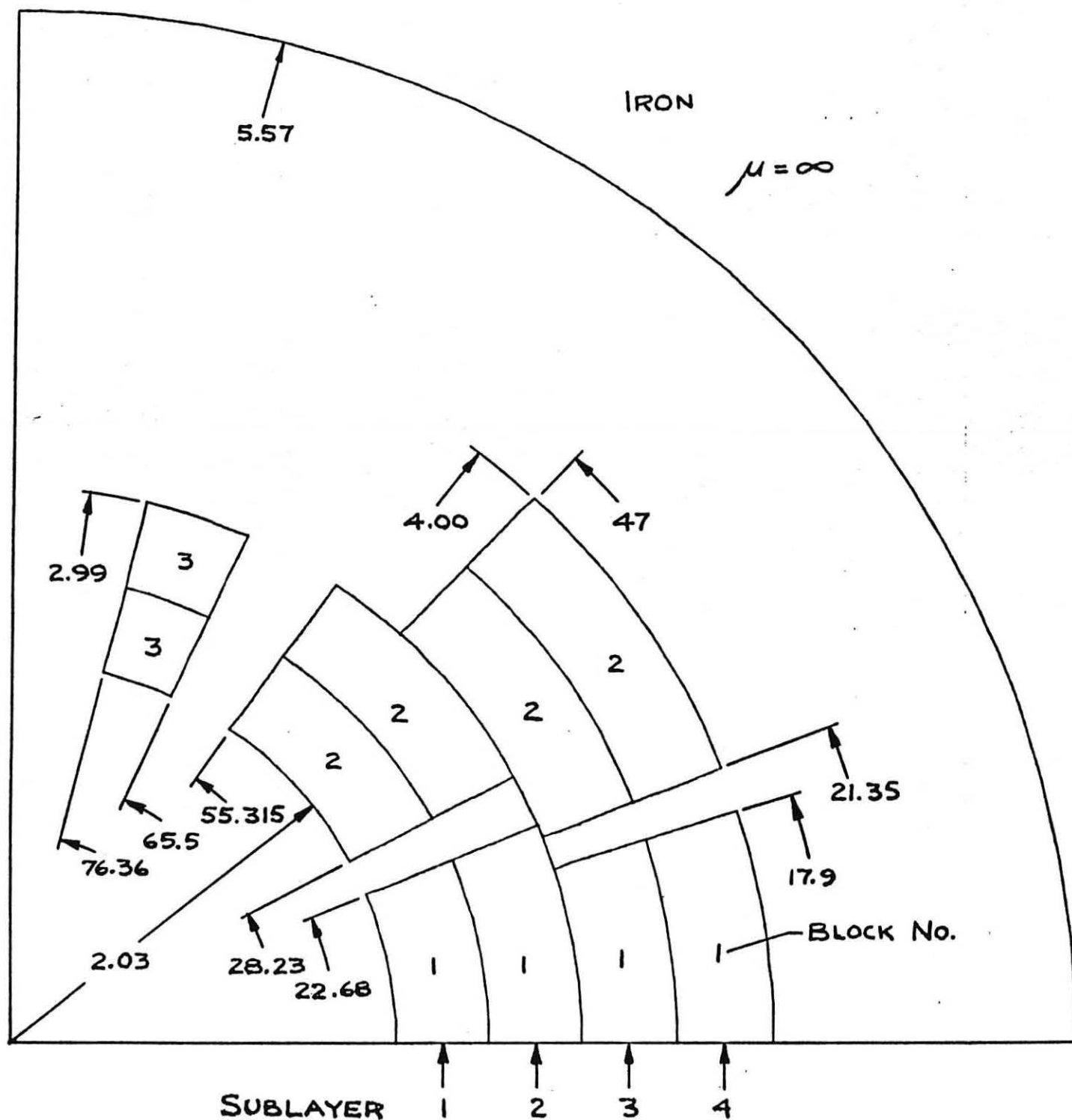
We next compare the measured sextupole and decapole moments of LBL-SSC model magnet D-12C-2 with those calculated by POISSON.

The inner and outer layers of the 4-cm bore two-layer magnet (Fig. 1) are made of a 23-strand and a 30-strand cable respectively, with 1.3 and 1.8 Cu/sc ratios. Stainless-steel collars over the outer layer displaced the iron to a radius of 5.57 cm. We have ignored possible saturation of the iron and therefore set the iron permeability to $\mu = \infty$ in these studies of magnetization effects. It is planned that the effect of images in iron of variable permeabilities will be checked in later work. Each individual layer has been subdivided in the computations into two parts of equal radial thickness in order to take care of the radial dependency of the current density and magnetization.

At the time this work was carried out only magnetization measurements for the inner layer were available to us. Such data took into account the existence of copper and superconductor only. We therefore took the steps necessary to scale this single magnetization curve so as to reflect the physical conditions in each of the sublayers as they exist during magnet operation. The full details of the calculations have been placed in Appendix A.

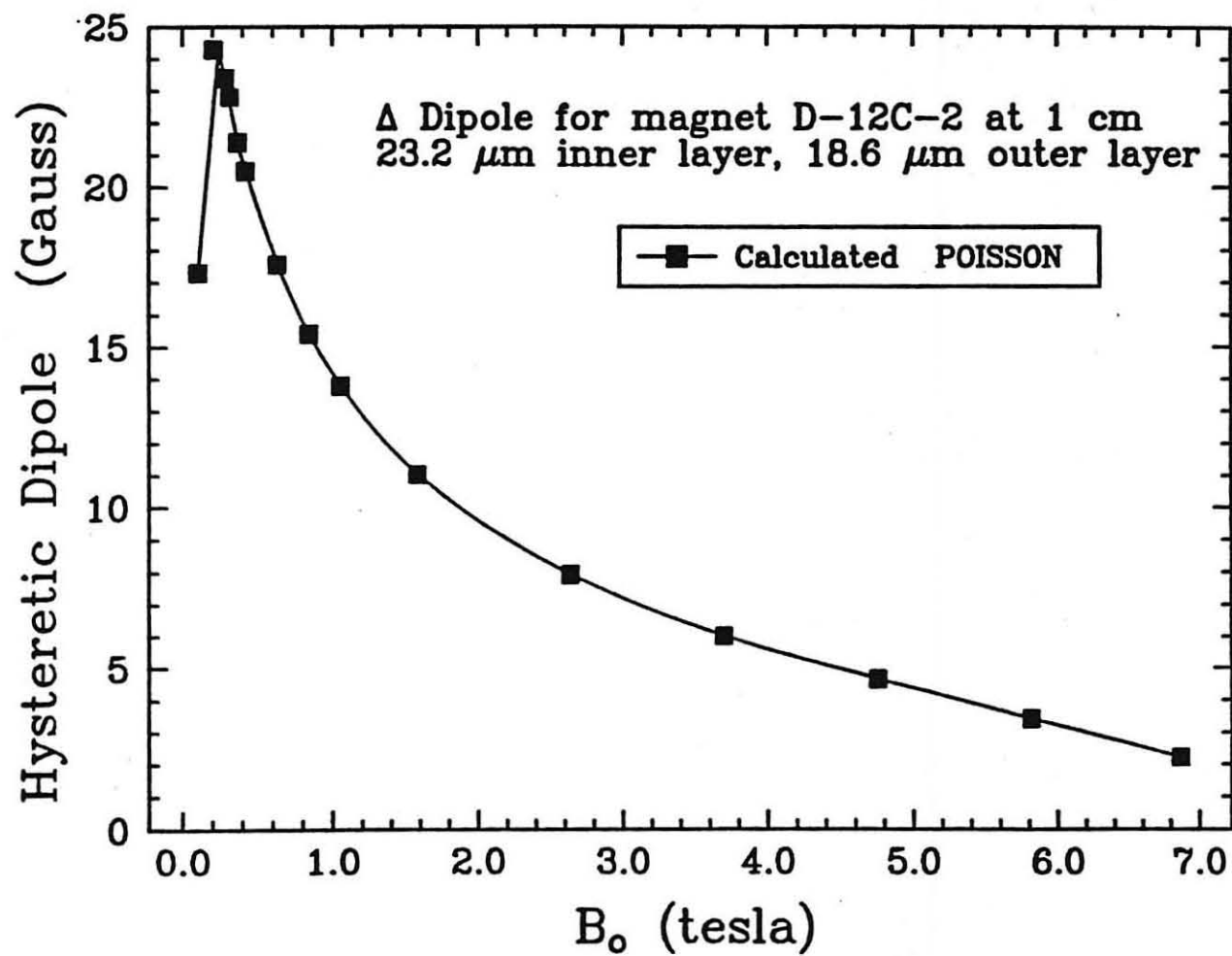
Results

A series of POISSON runs was made (total of 32) to produce data in the range of 0.1 T to 6.8 T. The first half of the runs employed magnetization tables corresponding



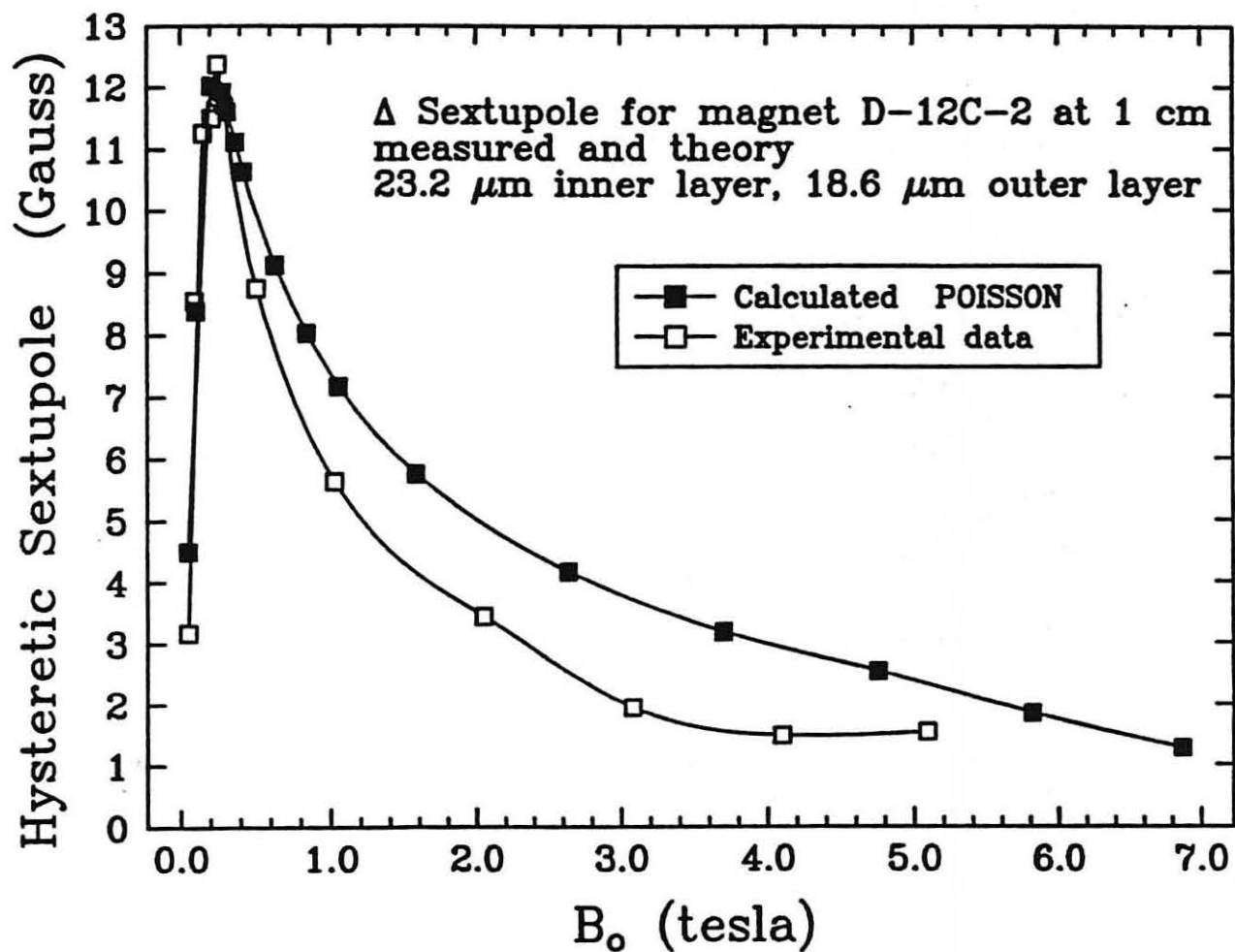
to an increase in current, and the remainder, for the same field interval, employed magnetization tables for decreasing current. At each field level we obtained two solutions such that upon subtracting their vector potential values we were left with a vector potential that corresponds to the total field change due to magnetization effects. The differential field harmonics (up minus down) were calculated and are plotted in Figs. 2-4. The individual sextupole and decapole coefficients for a full cycle (b_2 and b_4) are plotted in Figs. 5 and 6 (all harmonic calculations were performed at 1 cm radius). Flux lines during a current increase at 0.28 T are plotted in Fig. 7. The effect of magnetization for these two curves can scarcely be distinguished. In order to suppress the dominating transport current effect we accordingly have calculated the field assuming no magnetization ($\mu = 1$ in the current regions), and then subtracted the resulting vector potential from the vector potential at the same field when magnetization is present. Flux lines due to magnetization only are plotted in Fig. 8.

Δ Dipole for design D (4 cm)



XBL 858-3192

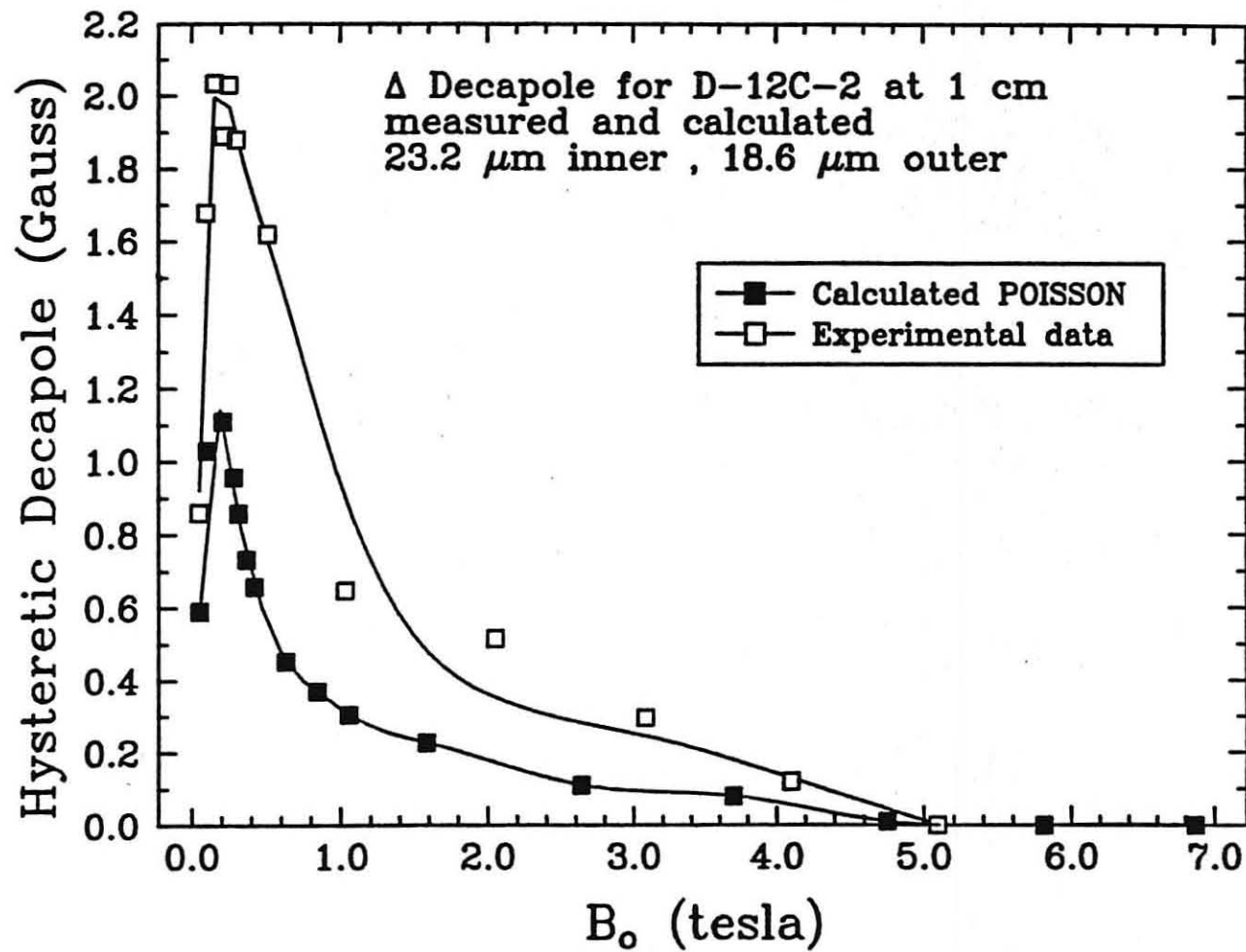
Fig. 2. Differential dipole component (up minus down) due to magnetization.

Δ Sextupole for design D (4 cm)

XBL 858-3189

Fig. 3. Differential sextupole component due to magnetization.

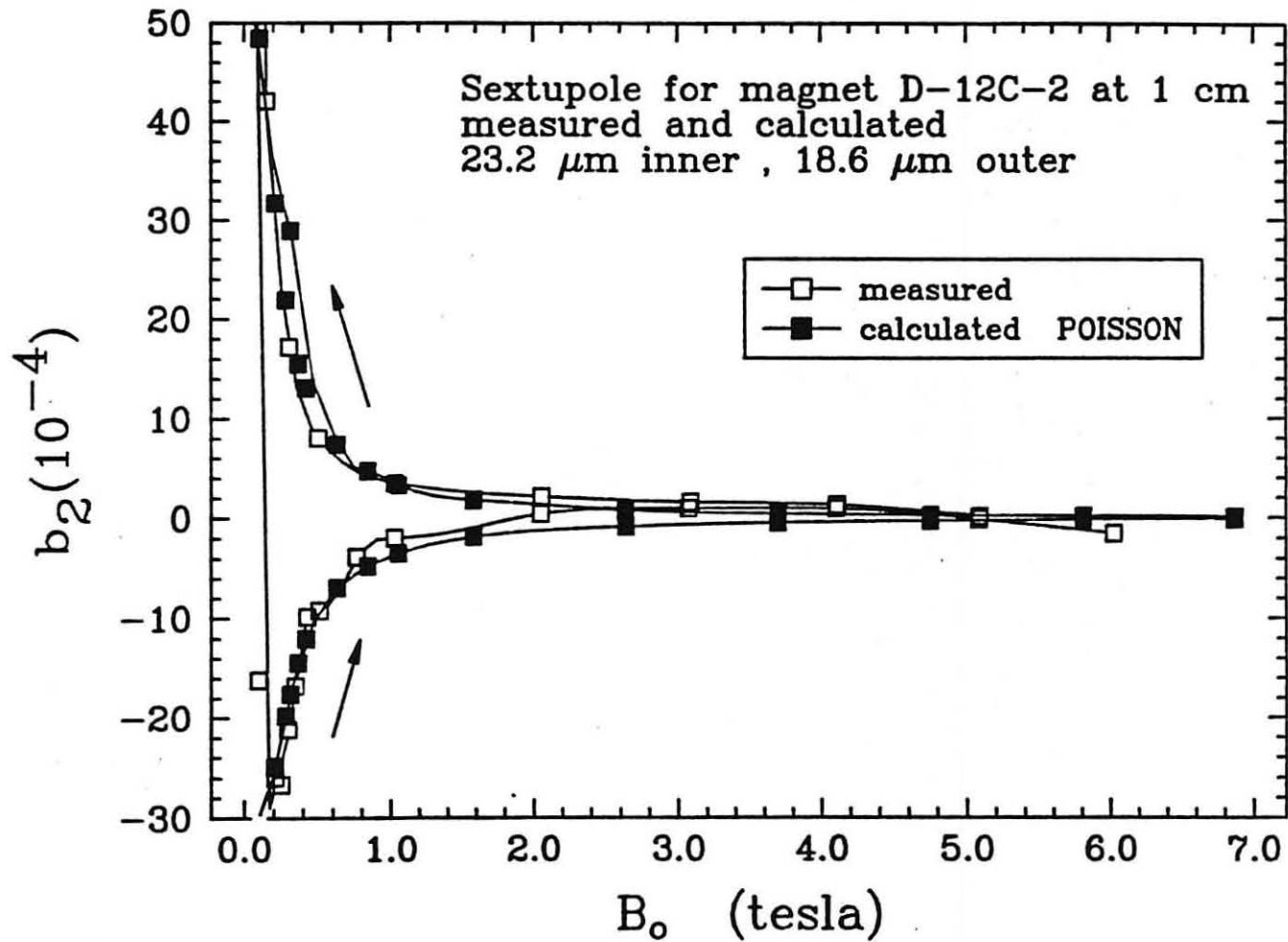
Δ Decapole for design D (4 cm)



XBL 858-3193

Fig. 4. Differential decapole component due to magnetization.

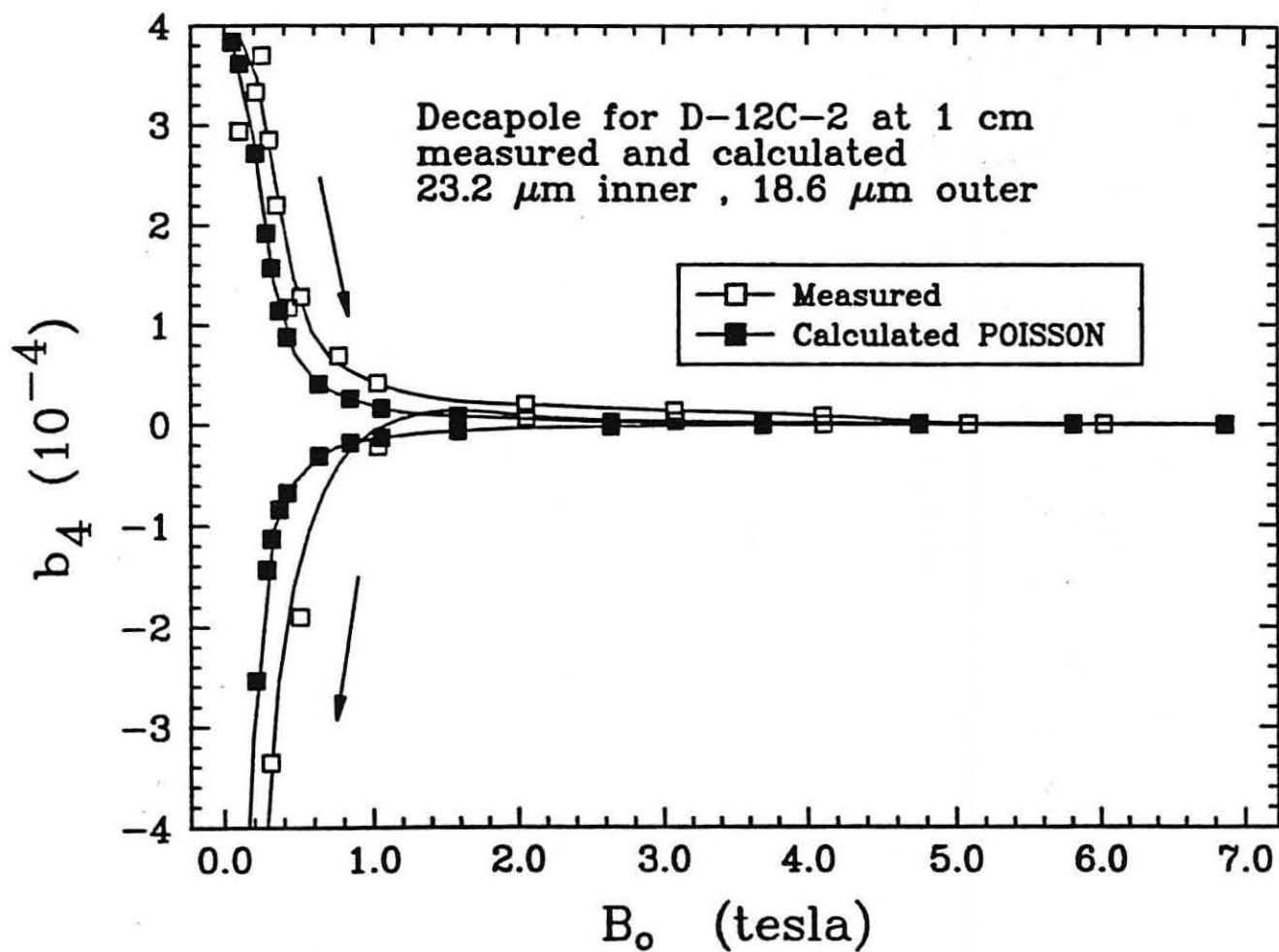
D-12C-2 Sextupole



XBL 858-3191

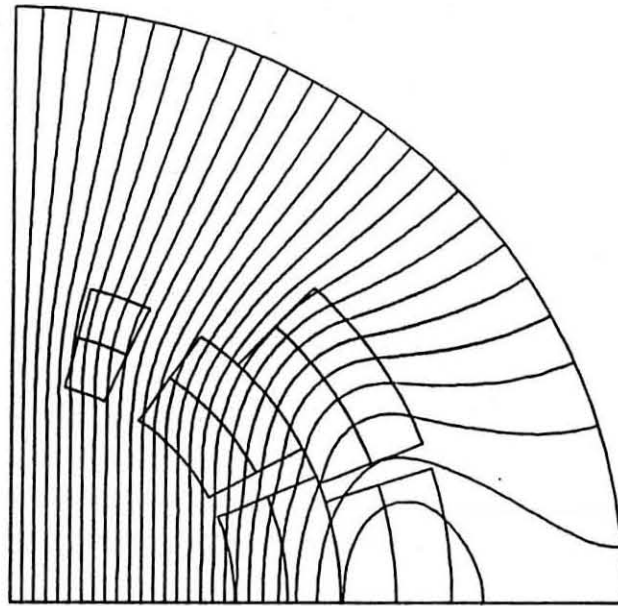
Fig. 5. Sextupole coefficient due to magnetization during a full field cycle.

D-12C-2 Decapole

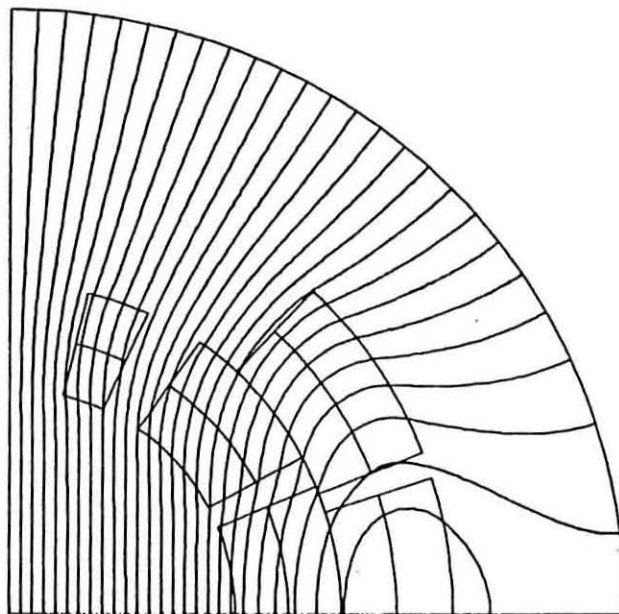


XBL 858-3190

Fig. 6. Decapole coefficient due to magnetization during a full field cycle.



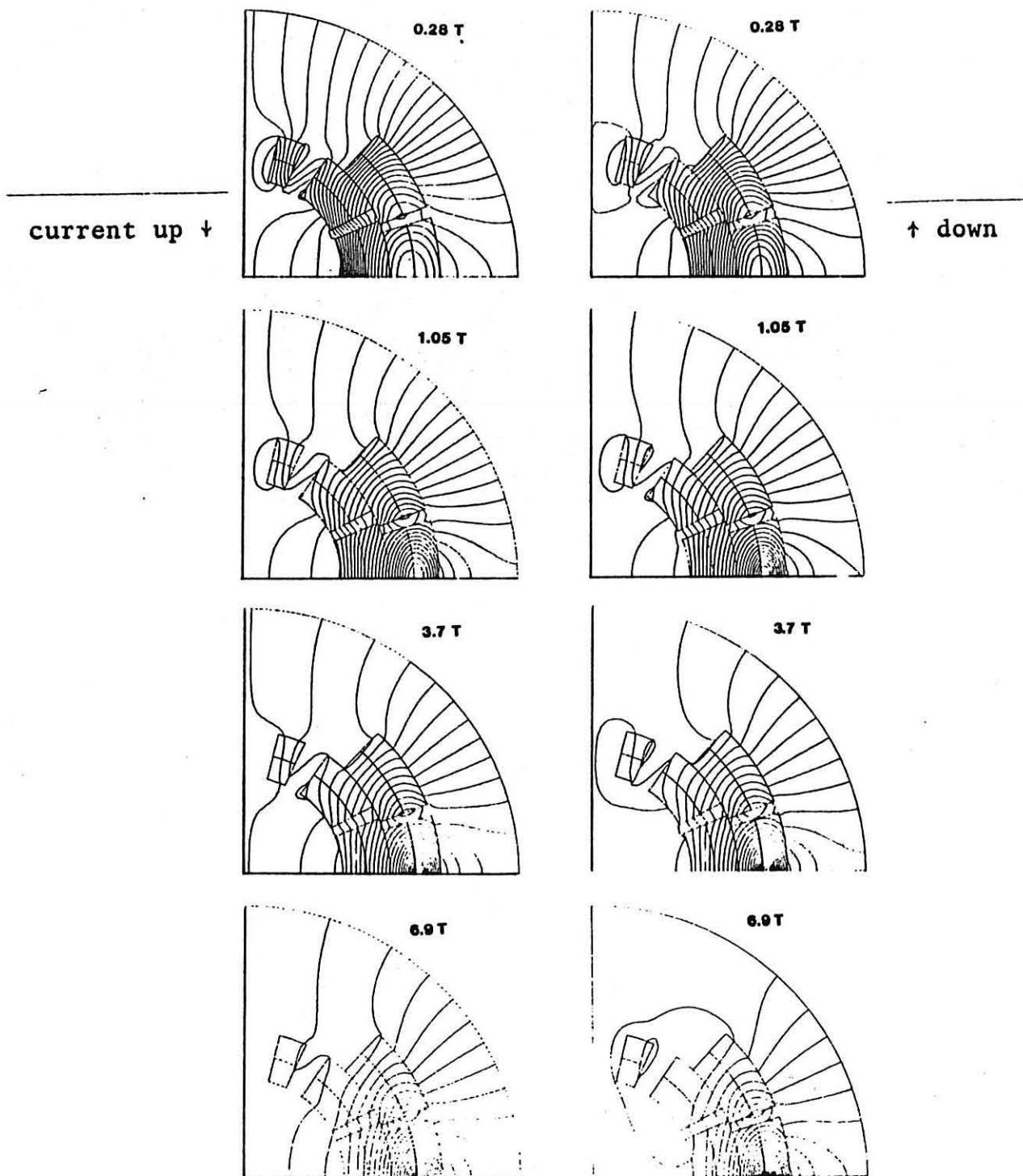
(a)



(b)

XBL 858-3195

Fig. 7. Flux lines during a current increase (a) and a current decrease (b), at 0.28 T. The effect of magnetization can scarcely be distinguished.



XBL 658-3106

Fig. 8. Flux lines due to magnetization only, at various field levels, produced by subtracting the vector potential which includes magnetization from the one that has zero magnetization.

APPENDIX A

Scaling Procedure

We shall be using the notation F_{ij} , where i corresponds to the type of scaling and j denotes the sublayer number.

- 1) Calculate F_{1j} , the ratio between the true copper and superconductor cross section area to that of the winding block. The amount of copper is as specified by the Cu/sc ratio for each sublayer.
- 2) Generate the critical current curve as a function of field and superpose the load line corresponding to the field at the windings. From the ratio δ between transport current and critical current (at a given field) calculate $F_{2j} = 1 - \delta$. It has been assumed that this curve is the same for all sublayers. Note that below 1.0 T, F_{2j} is substantially constant (≈ 1.0) and is independent of field, therefore B or H can be used as an independent variable; the distinction between B and H accordingly is not critical for describing the functional dependence of F_{2j} .
- 3) Use F_{3j} to scale for variations in filament size. This is the ratio between filament diameters.

Once scaling factors for each of the sublayers have been generated they should be consolidated into a single factor according to:

$$F_j = \prod_{i=1}^3 F_{ij}$$

The single original M-H curve can now be scaled into four different curves, MF_j vs. H , each corresponding to an individual sublayer.

Inner-Layer - SC #280

Filament diameter: $d_f = 23.2 \text{ } (\mu\text{m})$ (SC only)

Number of filaments: $N_f = 527$

Number of strands: $N_s = 23$

$R = 1.3:1$ Cu/sc

Strand current density at 5 T is: $J_c \approx 2200 \text{ A/mm}^2$

The strand diameter is: $D_s = d_f \sqrt{N_f(1+R)}$

$$D_s = 8.077 \times 10^{-4} \text{ (m)} = 31.8 \text{ (mil)}$$

Strand cross section area:

$$A_s = \frac{\pi D_s^2}{4} = 5.124 \times 10^{-3} \text{ (cm}^2\text{)}$$

Cable cross section area (including Cu):

$$A_c = N_s \cdot A_s = 0.117847 \text{ (cm}^2\text{)}$$

Outer-Layer - SC #293

Filament diameter: $d_f = 18.6 \text{ } (\mu\text{m})$

Number of filaments: $N_f = 434$

Number of strands:

$$N_s = 30$$

$$R = 1.8:1 \text{ Cu/sc}$$

Strand current density at 5 T is:

$$J_c = 2400 \text{ A/mm}^2$$

The strand diameter is:

$$D_s = 6.484 \times 10^{-4} \text{ (m)} = 25.53 \text{ (mil)}$$

and cross section area:

$$A_s = 3.302 \times 10^{-3} \text{ (cm}^2\text{)}$$

Cable cross section area (including Cu):

$$A_c = 0.09906 \text{ (cm}^2\text{)}$$

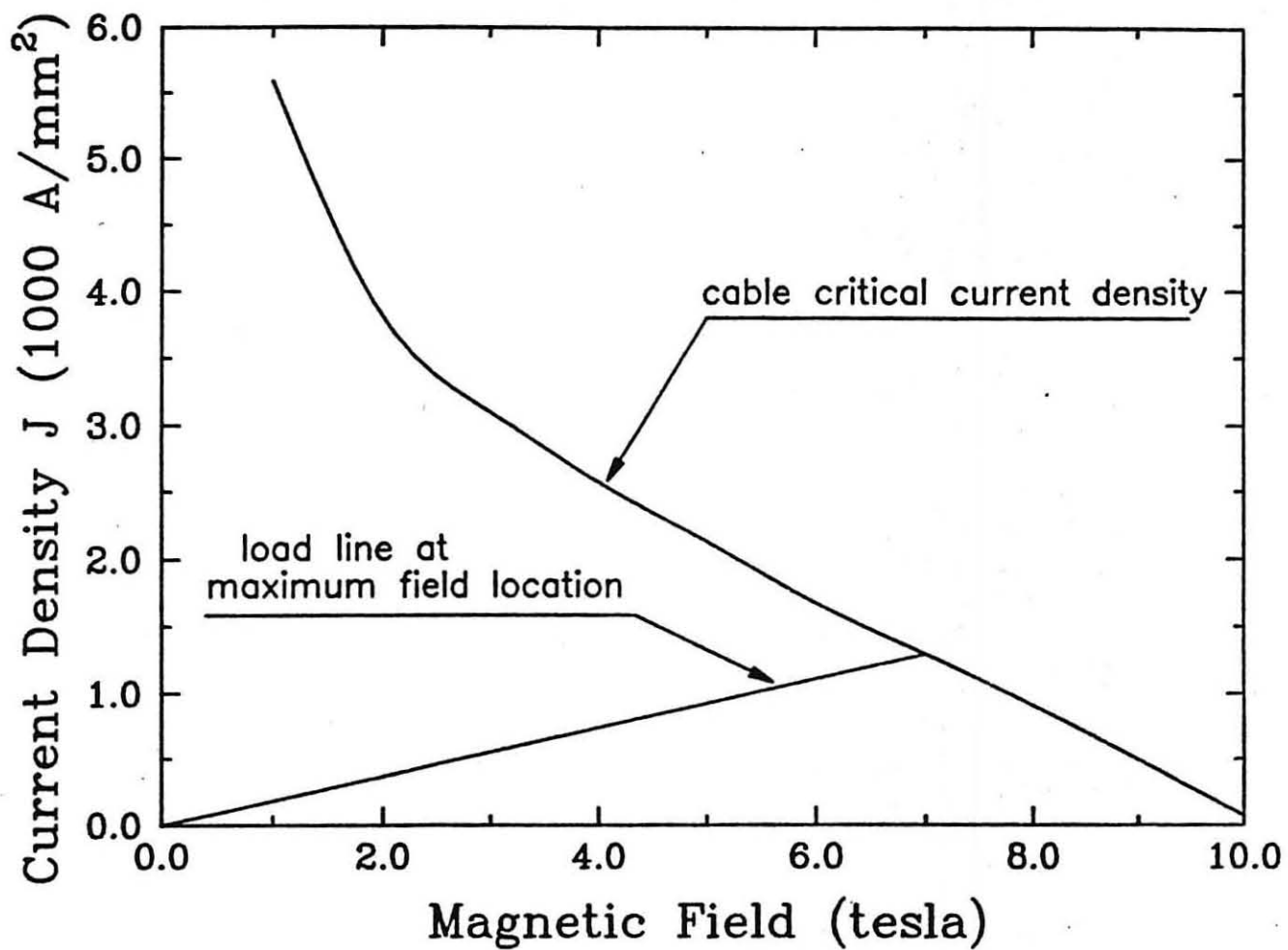
F_{1j}

Below is a table used to calculate the scale factor F_{1j} associated with the cross sectional area ratio between the copper + superconductor and the block conductor area (see Fig. 1 in the main text).

F_{2j}

We have calculated the magnetization scale factor associated with transport current. We have scaled both layers based on the J_c -B curve for the inner layer only. Plotted in Fig. 9 is the load line curve for magnet D-12C-2 and the cable critical current density curve (data for this curve were provided by short sample and magnetization measurements).

Sublayer	Location	Block area A_B (cm ²)	N'_S # of strands	Area of Cu+sc (cm ²) $A'_S = N'_S A_S$	A'_S/A_B	F_{1j}
1	1	0.4313	11.5	0.3535	0.820	0.825
1	2	0.5151	11.5	0.41246	0.8007	0.825
1	3	0.2064	11.5	0.17677	0.85644	0.825
2	1	0.5225	11.5	0.3535	0.6766	0.680
2	2	0.6240	11.5	0.41246	0.6610	0.680
2	3	0.2502	11.5	0.17677	0.7065	0.680
3	1	0.5115	15	0.39624	0.7746	0.790
3	2	0.7330	15	0.59436	0.811	0.790
4	1	0.5913	15	0.39624	0.67011	0.680
4	2	0.8471	15	0.59436	0.7016	0.680

Magnet D-12C-2

XBL 858-3194

Fig. 9. Critical current density curve for inner-layer cable.

B(T)	$I_{ss}^{(A)}$	$I_t^{(A)}$	$\delta = \frac{I_t}{I_{ss}}$	$F_{2j} = 1-\delta$
0.5	42000	473	0.0112	0.988
1.0	32000	945	0.02937	0.9706
2.0	21110	1891	0.08957	0.9104
3.0	17216	2837	0.1648	0.835
4.0	13988	3782	0.27	0.7296
5.0	11273	4728	0.4194	0.5806
6.0	8557	5673	0.6629	0.337
7.0	6605	6605	1.0	0

We have plotted F_{2j} as a function of B in Fig. 10 and used the following curve fit.

$$F_{2j} = 1-\delta = -5.806 \times 10^{-4} B^4 + 5.06 \times 10^{-3} B^3 - 2.564 \times 10^{-2} B^2 - 1.3295 \times 10^{-2} B + 1.0003 .$$

Errors in F_{2j} are of the order of 4%.

We have scaled J_c at low B and M at high B using the relation:

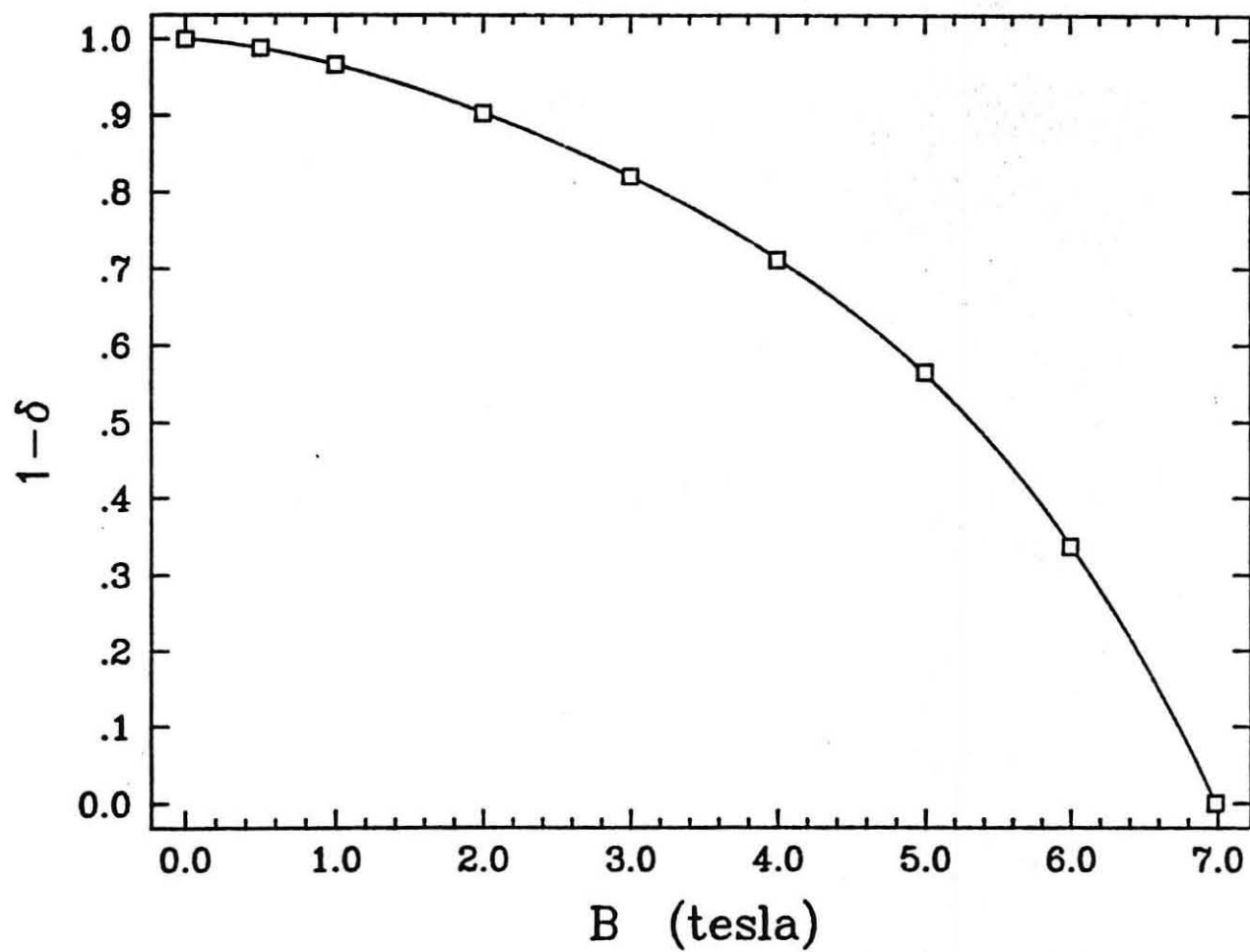
$$2\mu_0 M = 2\mu_0 \frac{2}{3\pi} \lambda J_c(H) d$$

$d \equiv$ filament diameter

$\lambda \equiv$ volume fraction of SC; $1/(1+R)$

$$2\mu_0 M = M^{up} - M^{down}$$

Transport current correction



XBL 858-3188

Fig. 10. Magnetization scaling factor due to transport current.

B(T)	j_c (A/mm ²)	Calculated $2\mu_0 M$ (mT)	2 measured (mT)	$\frac{\text{measured}}{\text{calculated}}$	Extrapolated (mT)
1.0	5590±12%	30.85±3.8	27.0	0.875	27.0
2.0	3810±8%	21.02±1.7	18.8	0.894	18.8
3.0	3095±8%	17.08±1.5	15.0	0.88	15.0
4.0	2565±6%	14.15±0.92			12.45
5.0	2125±3%	11.72±0.41			10.31
6.0	1670	9.21			8.10
7.0	1290	7.12			6.26

F_{3j}

This scaling factor reflects variations in filament diameter. Since the measured magnetization curve of the inner layer was used, we have $F_{3_{\text{inner}}} = 1.0$. In scaling the outer layer (18.6 μm filament diameter) from a 23.2 μm filament diameter of the inner layer we have $F_{3_{\text{outer}}} = 18.6/23.6 = 0.802$.

Input to POISSON

A suitable input to POISSON requires a B-H or B- γ table ($\gamma = 1/\mu$). We have decided on a B- γ table. For the original M-H curve we can write:

$$B = H + M$$

or

$$B = \left(1 + \frac{M}{H}\right) H.$$

With

$$\mu_{\text{or}} = 1 + \frac{M}{H}; \quad (\text{or} = \text{original})$$

ORIGINAL MAGNETIZATION TABLE FROM GHOSH 23.2 μ m 1.3:1 SC

UP
H (Gauss) $\gamma = \frac{1}{\mu}$

21.8	.047
43.6	0.104
148.0	0.3229
292.0	0.5835
476.0	0.823
580.0	0.9868
702.7	1.1218
890.0	1.1793
1139.0	1.2050
1414.0	1.2048
1580.0	1.2018
1846.0	1.17519
2029.0	1.1621
2243.0	1.1421
2544.7	1.1183
2815.0	1.10096
3199.0	1.084
3766.9	1.064
4395.4	1.0495
5220.0	1.03829
6010.0	1.03088
7010.0	1.02488
8262.7	1.0197
9166.0	1.016766
9969.4	1.0146
12219.7	1.0105
14681.0	1.00796
17775.8	1.005766
21485.7	1.00446
25846.0	1.003159
30153.8	1.00249
35358.2	1.00205
40000.0	1.0015
50000.0	1.0010
60000.0	1.00067
70000.0	1.00045

DOWN

17.45	.03775
283.7	0.408
541.24	0.5921
811.87	0.70645
1235.2	0.8015
1772.15	0.86623
2636.4	0.9167
3208.2	0.934977
4430.0	0.957
5914.45	0.9715
7215.2	0.9787
8651.2	0.98389
9952.0	0.98686
11622.0	0.98957
13696.7	0.99169
16105.5	0.99363
18883.5	0.99503
22083.5	0.99601
26795.6	0.997137
29661.5	0.997477
32879.1	0.997918
35006.6	0.998281
40000.0	0.99844
50000.0	0.99897
60000.0	0.999325
70000.0	0.99955

$$B = \mu_{or} H . \quad (1)$$

The permeability of the scaled magnetization is written as:

$$\mu_{sj} = 1 + \frac{MF_j}{H} ;$$

or

$$\mu_{sj} = 1 + (\mu_{or}-1) F_j .$$

In terms of γ we have:

$$\gamma_{sj} = \frac{1}{1 + \left(\frac{1}{\gamma_{or}} - 1 \right) F_j}$$

and

$$B = \left(\frac{1}{\gamma_{sj}} \right) H$$

Note that the parameters γ_{sj} are H dependent.

The F_j calculated for the four sublayers are:

$$F_1 = 0.825 \quad F_3 = 0.633$$

$$F_2 = 0.680 \quad F_4 = 0.545$$

at low field strengths, but at higher fields the factors F_{2j} that contribute to these quantities will introduce some field dependence. The original and scaled magnetization curves are included here both in tabular form, and as plotted curves, Fig. 11.

Several restrictions in input entries to POISSON are noted.

B	$\gamma = \frac{1}{\mu}$
0.0	1.163
979.327	1.163043
1216.02	1.162809
1361.53	1.160455
1619.51	1.139848
1796.15	1.129636
2013.52	1.113972
2323.50	1.095199
2603.03	1.081430
2995.66	1.067878
3581.36	1.051808
4225.98	1.040090
5063.13	1.030982
5863.74	1.024944
6872.32	1.020035
8134.28	1.015788
9044.95	1.013383
9854.98	1.011610
12119.7	1.008250
14591.1	1.006159
17698.5	1.004365
21415.5	1.003278
25788.5	1.002231
30103.2	1.001680
35312.5	1.001295
39963.3	1.000917
49976.1	1.000479
59988.7	1.000188
70000.0	1.000000

B	$\gamma = \frac{1}{\mu}$
0.0	1.130
1007.39	1.130643
1250.82	1.130461
1399.93	1.128627
1659.32	1.112504
1837.08	1.104471
2053.85	1.092096
2362.38	1.077176
2640.29	1.066171
3031.40	1.055289
3613.97	1.042317
4255.76	1.032813
5090.70	1.025399
5889.45	1.020470
6896.51	1.016455
8156.85	1.012977
9066.22	1.011005
9875.09	1.009550
12137.3	1.006790
14606.9	1.005071
17712.1	1.003596
21427.8	1.002700
25798.6	1.001838
30112.1	1.001384
35320.5	1.001067
39969.8	1.000756
49980.3	1.000395
59990.7	1.000155
70000.0	1.000000

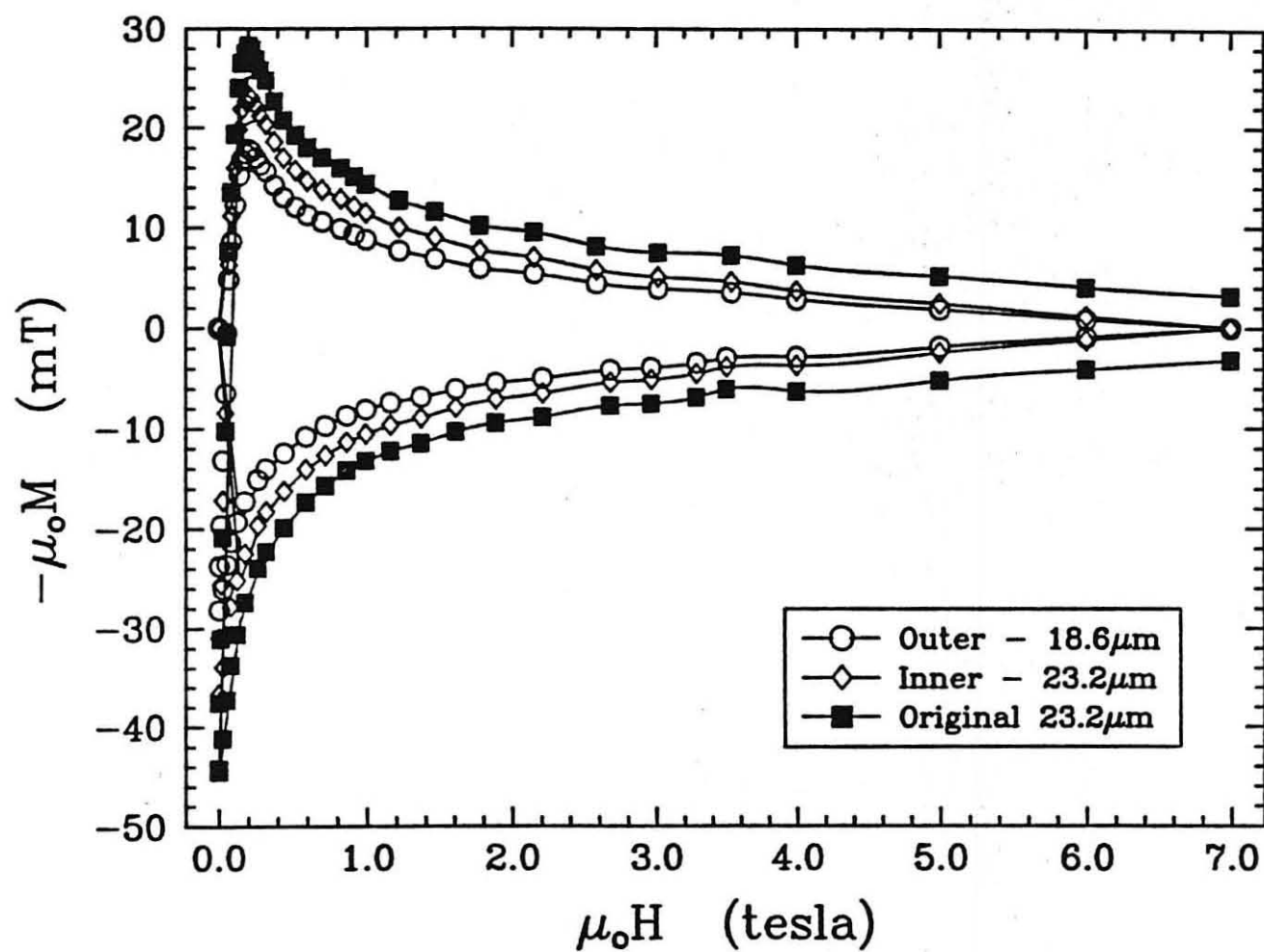
B	$\gamma = \frac{1}{\mu}$
0.0	1.10
1033.52	1.102060
1283.21	1.101921
1435.68	1.100524
1696.38	1.088198
1875.18	1.082029
2091.40	1.072487
2398.58	1.060921
2674.97	1.052347
3064.67	1.043831
3644.33	1.033633
4283.48	1.026129
5116.37	1.020254
5913.38	1.016340
6919.04	1.013146
8177.86	1.010374
9086.03	1.008801
9893.81	1.007640
12153.7	1.005435
14621.6	1.004060
17724.8	1.002880
21439.3	1.002163
25808.0	1.001473
30120.4	1.001109
35328.0	1.000855
39975.8	1.000606
49984.2	1.000316
59992.6	1.000124
70000.0	1.000000

B	$\gamma = \frac{1}{\mu}$
0.0	.75
1486.99	.8306738
1997.15	.8873403
2832.95	.9306197
3390.97	.9461023
4592.43	.9646310
6055.27	.9767445
7341.95	.9827359
8764.78	.9870416
10057.5	.9895065
11718.7	.9917520
13786.1	.9935144
16184.6	.9951109
18954.3	.9962648
22148.2	.9970806
26849.4	.9979968
29712.4	.9982883
32923.9	.9986408
35044.8	.9989090
40036.7	.9990839
50023.9	.9995224
60011.3	.9998121
70000.0	1.000000

B	$\gamma = \frac{1}{\mu}$
0.0	.78
1442.73	.8561532
1957.60	.9052652
2798.41	.9421079
3358.84	.9551504
4563.88	.9706649
6030.52	.9807531
7319.67	.9857268
8744.81	.9892948
10039.0	.9913348
11701.7	.9931918
13770.4	.9946482
16170.7	.9959668
18941.9	.9969194
22136.8	.9975923
26839.9	.9983484
29703.4	.9985887
32916.0	.9988793
35038.1	.9991006
40030.2	.9992448
50019.7	.9996063
60009.3	.9998450
70000.0	1.000000

B	$\gamma = \frac{1}{\mu}$
0.0	0.80
995.442	.8155876
1401.53	.8813218
1920.79	.9226174
2766.24	.9530616
3328.94	.9637315
4537.30	.9763511
6007.48	.9845151
7298.93	.9885279
8726.23	.9914019
10021.7	.9930431
11685.8	.9945362
13755.8	.9957062
16157.8	.9967649
18930.3	.9975294
22126.2	.9980694
26831.1	.9986757
29695.1	.9988686
32908.7	.9991015
35031.9	.9992790
40024.2	.9993945
50015.8	.9996845
60007.5	.9998758
70000.0	1.000000

Magnetization Curves D-12C-2



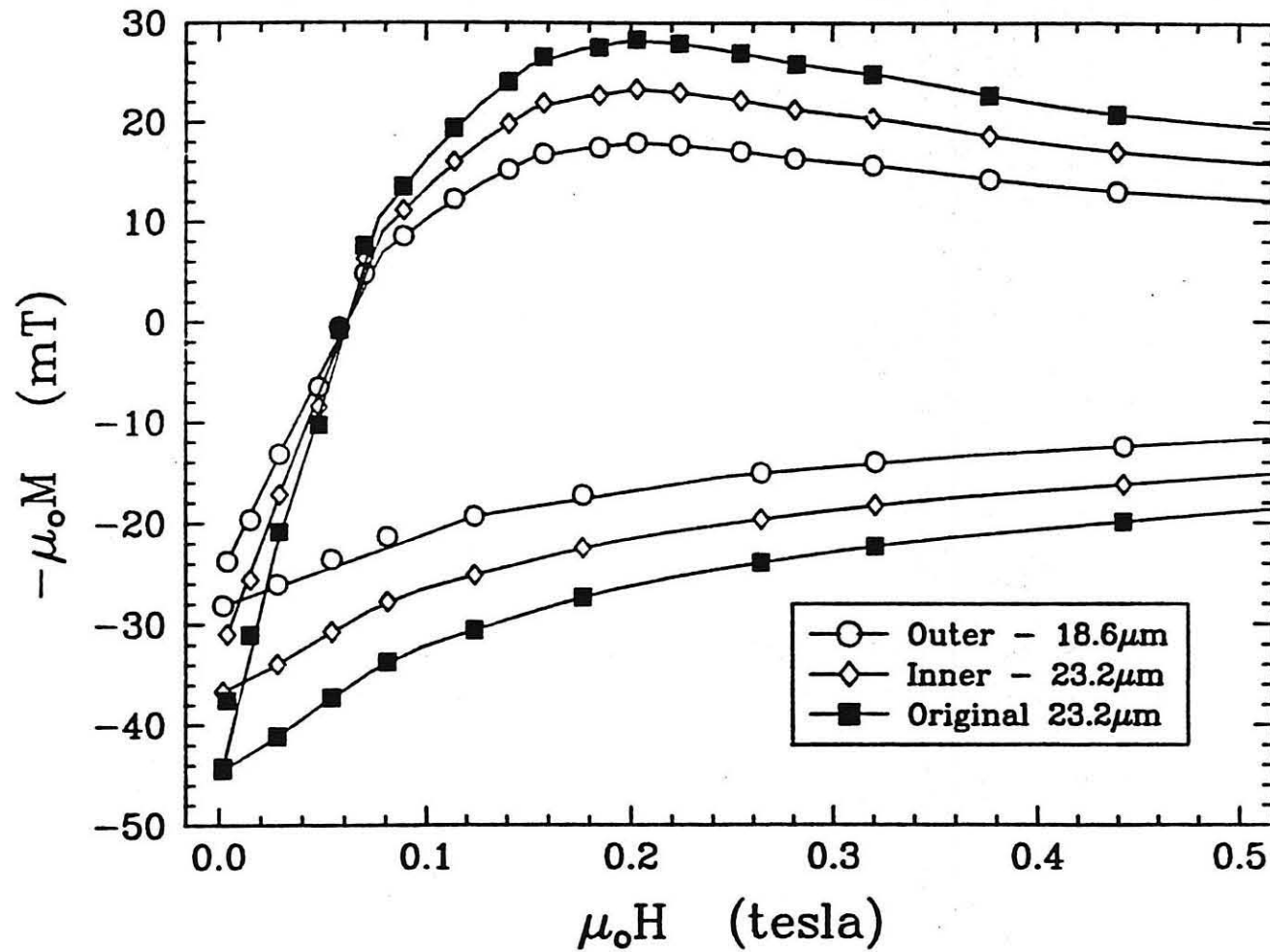
XBL 858-3187

Fig. 11. Some of the magnetization curves used in the present calculations.

POISSON is restricted in the number of permeability tables it can accept. Excluding the built-in table, up to three additional tables can be entered. This condition can be relaxed through the use of the POISSON stacking factor. We decided, however, to limit magnetization entries in the present work to three tables and therefore substituted F_2 for F_3 .

The second and the most troublesome entry to POISSON arises from following this technique at low fields ($H < 300$ Gauss), where double values of γ vs. B can then occur. Since POISSON does not support B entries in a permeability table which are less than zero we were forced to approximate the table entries at low fields. An adjustment to the M - H curve at low field (Fig. 12) was made so that at $H = 0$, $M = 0$ (Fig. 13). This was done by drawing a linear asymptote from the origin to the upper curve and adjusting the lower curve analogously by drawing a linear curve from the origin over the same field interval.

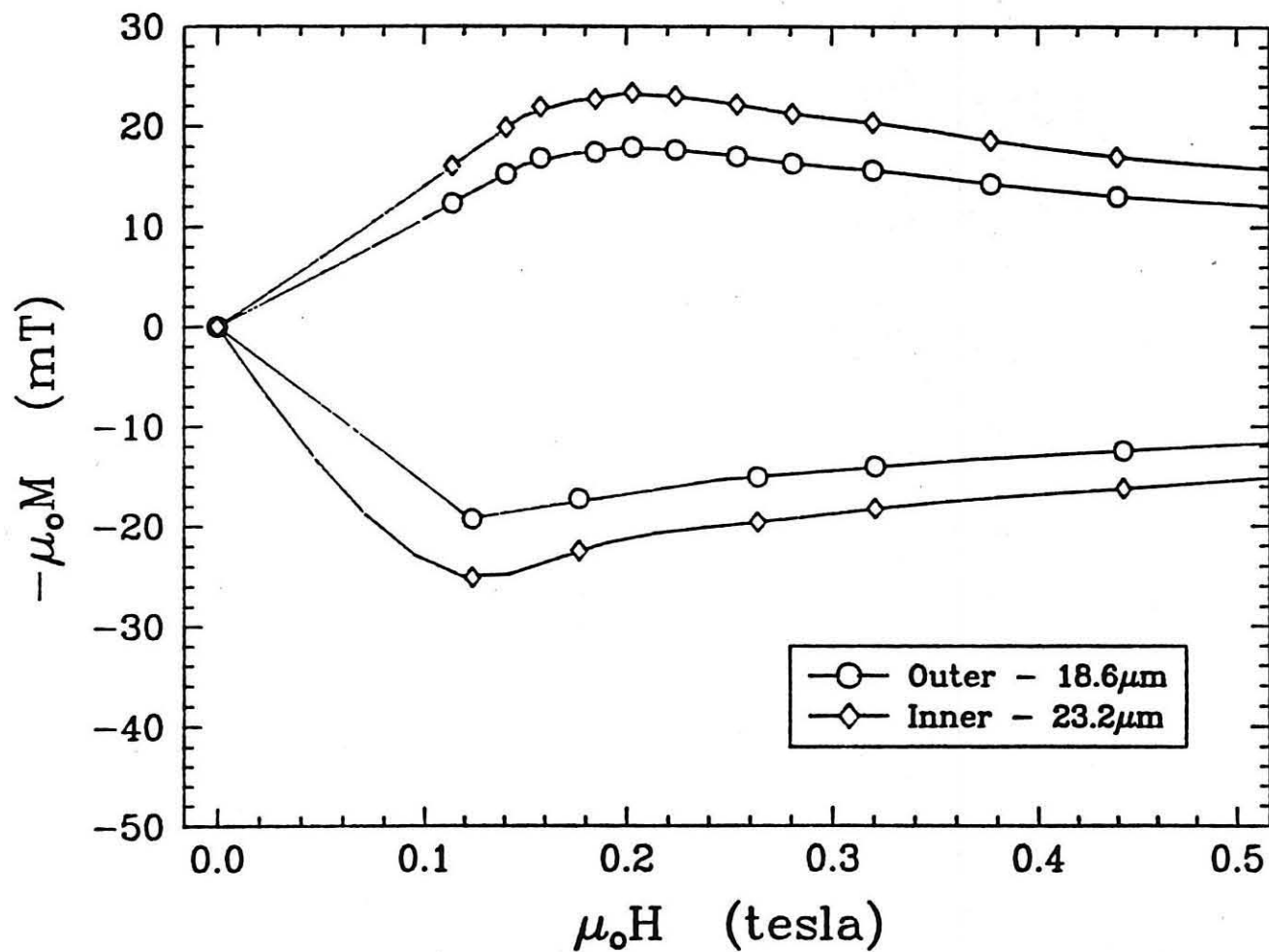
Magnetization Curves D-12C-2



XBL 858-3186

Fig. 12. The low field magnetization values as derived from scaling.

Magnetization Curves D-12C-2
As used in POISSON



XBL 858-3185

Fig. 13. Low field magnetization adjustment as introduced to POISSON.